Experimental characteristics of indoor wideband MIMO radio channels and their impact on stochastic modelling

Steinböck, Gerhard; Yin, Xuefeng; Pedersen, Troels; Fleury, Bernard Henri

Published in:
Digital Signal Processing Workshop and 5th IEEE Signal Processing Education Workshop, 2009. DSP/SPE 2009. IEEE 13th

DOI (link to publication from Publisher):
10.1109/DSP.2009.4785939

Publication date:
2009

Document Version
Publisher's PDF, also known as Version of record

EXPERIMENTAL CHARACTERISTICS OF INDOOR WIDEBAND MIMO RADIO CHANNELS AND THEIR IMPACT ON STOCHASTIC MODELLING

Gerhard Steinböck[1], *Xuefeng Yin*[1,2], *Troels Pedersen*[1] *and Bernard H. Fleury*[1,3]

Aalborg University[1], Department of Electronic Systems, Aalborg, Denmark
Tongji University[2], College of Electronics and Information Technologies, Shanghai, China
Telecommunications Research Center Vienna (ftw.)[3], Vienna, Austria

ABSTRACT

We compare two methods for estimation of path-component spreads in bi-azimuth and delay, namely the clustering approach and the density approach, in indoor environments. Monte Carlo simulations reveal possible shortcomings of the clustering approach. Published estimates of component spreads in delay, azimuth of departure and azimuth of arrival obtained with the clustering approach are reviewed and contrasted with estimates gathered using the density approach. A detailed study of these experimental data, aided with the insight gained from the simulation results, leads to the conjecture that in some cases the estimated spreads computed with the clustering approach are too large. The settings of the path component spreads of two widely used models including bi-azimuth delay dispersion, namely the Winner II Model and the 802.11 Tgn Model are revisited based on these findings. The investigations stress the obvious, but apparently sometimes forgotten, importance of validating the behavior and performance of channel parameter estimation techniques before using these tools to extract empirical information from measurement data.

1. INTRODUCTION

The response of the radio channel is commonly modeled as a superposition of a number of "path components". Each of these components represents the contribution of some electromagnetic wave, propagating from the transmitter to the receiver via a specific propagation path. Along this path the wave may interact with a number of objects called "scatterers". The path components may be dispersive in delay, direction of departure (DoD), direction of arrival (DoA), Doppler frequency and in polarizations, due to the electromagnetic and geometric properties of the scatterers (see Fig. 1). In the sequel, we refer to these dimensions as dispersion dimensions. In [1–3] it is stressed that stochastic models need to include the dispersive behavior of individual path components in order to accurately emulate real propagation channels.

This work was supported by the ICT-216715 FP7 Network of Excellence in Wireless COMmunication (NewCom++) and by the project ICT-217033 Wireless Hybrid Enhanced Mobile Radio Estimators (WHERE). The Telecommunications Research Center Vienna (ftw) is supported by the Austrian Government and the City of Vienna in the competence center program COMET.

The Bartlett spectral estimator [4] is widely used to assess dispersion of the radio channel in DoA, DoD or jointly in both directions. The direction or bi-direction Bartlett spectrum usually provides a good insight into the distribution of dominant path components, especially in wide-band scenarios, when it is computed as a function of the delay. Indeed, the nominal values, or centers of gravity, of these components in these dimensions can usually be assessed with a reasonable accuracy. The Bartlett spectrum is, however, not appropriate to assess the dispersive behavior of these individual components, because the spreads of these components are typically below the resolution of practical antenna arrays.

High resolution methods rely on parametric models that aim at circumventing the impact of the system response by exploiting certain assumptions on the channel property. In our particular application it is assumed that waves can be considered as planar and specular, or nearly specular, over small regions including the transmit and receive arrays. Two main approaches for characterization of dispersive path components have been proposed in the literature. The first approach uses density functions to describe the power spectral density of dispersive path components and directly estimates the parameters of these density functions [5–10]. We refer to this approach as the "density approach". The second, so-called "clustering approach", attempts to approximate the dispersive path components by superpositions of specular components [11–15]. In a first stage a feasible high-resolution technique, commonly based on the SAGE (Space Alternating Generalized Expectation-maximization) algorithm [16], is applied on measurement data to estimate the characteristics of these specular components. In a second stage the estimated components undergo a manual or automated pruning process based on a predetermined selection criterion. Those components retained are grouped in "clusters", each cluster representing an individual dispersive path component. The dispersion characteristics of each dispersive path component, i.e. nominal values and spreads, are then extracted from the parameters of the specular components in the corresponding cluster.

The paper is organized as follows. The signal model of the radio channel including dispersive path components is introduced in Section 2. Section 3 gives a short literature review of previous works on the clustering and density approaches.

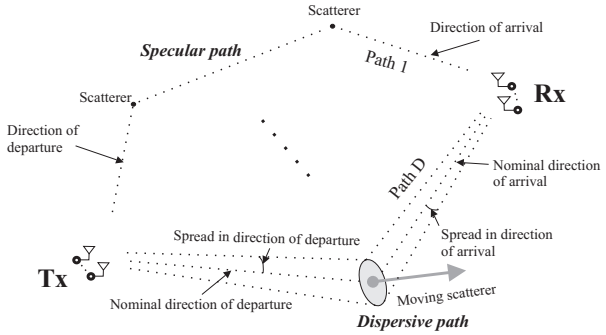

Fig. 1. Schematic representation of multipath propagation.

The performances of the clustering and density approaches are investigated in Section 4. This section also reviews values of component spreads obtained experimentally with both approaches, as well as such values specified in two widely used channel models including bi-azimuth-delay dispersion. Concluding remarks are stated in Section 5.

2. SIGNAL MODEL

We consider the propagation environment depicted in Fig. 1. The components of the complex baseband signal vector $\mathbf{s}(t) \in \mathbb{C}^{M_1}$ are fed to the inputs of the M_1 transmit antennas. The signals radiated by these antennas propagate via D paths to the M_2 receive antennas. The signal $\mathbf{Y}(t) \in \mathbb{C}^{M_2}$ at the outputs of these antennas reads [9]

$$\mathbf{Y}(t) = \int_{-\infty}^{\infty} \int_{\mathbb{S}_2} \int_{\mathbb{S}_2} \mathbf{c}_2(\mathbf{\Omega}_2)\mathbf{c}_1(\mathbf{\Omega}_1)^T \mathbf{s}(t-\tau) \\ h(\mathbf{\Omega}_1, \mathbf{\Omega}_2, \tau) d\mathbf{\Omega}_1 d\mathbf{\Omega}_2 d\tau + \mathbf{W}(t), \quad (1)$$

where τ is the propagation delay and $\mathbf{c}_i(\mathbf{\Omega}_i)$ is the response in direction $\mathbf{\Omega}_i$ of the transmit ($i = 1$) or the receive ($i = 2$) array. Here, $(\,\cdot\,)^T$ denotes the transpose operation. A direction $\mathbf{\Omega}$ is an element of the unit sphere $\mathbb{S}_2$. It is specified by its azimuth $\phi \in [-\pi, \pi)$ and co-elevation $\theta \in [0, \pi]$ according to $\mathbf{\Omega} = [\cos(\phi)\sin(\theta), \sin(\phi)\cos(\theta), \cos(\theta)]^T$. The noise vector $\mathbf{W}(t) \in \mathbb{C}^{M_2}$ is a spatially and temporarily white circularly symmetric complex Gaussian process.

It is assumed that the bi-direction-delay spread function $h(\mathbf{\Omega}_1, \mathbf{\Omega}_2, \tau)$ of the radio channel can be decomposed into D uncorrelated (or orthogonal) processes:

$$h(\mathbf{\Omega}_1, \mathbf{\Omega}_2, \tau) = \sum_{d=1}^{D} h_d(\mathbf{\Omega}_1, \mathbf{\Omega}_2, \tau). \quad (2)$$

Each process is meant to be contributed by a wave propagating along a specific propagation path. Assuming that the D processes in (2) are uncorrelated, the bi-direction-delay power spectrum is of the form

$$P(\mathbf{\Omega}_1, \mathbf{\Omega}_2, \tau) = \mathbb{E}\left[\left|h(\mathbf{\Omega}_1, \mathbf{\Omega}_2, \tau)\right|^2\right] \quad (3)$$

$$= \sum_{d=1}^{D} P_d(\mathbf{\Omega}_1, \mathbf{\Omega}_2, \tau), \quad (4)$$

where $\mathbb{E}\,[\,\cdot\,]$ denotes the expectation operator and

$$P_d(\mathbf{\Omega}_1, \mathbf{\Omega}_2, \tau) = \mathbb{E}\left[\left|h_d(\mathbf{\Omega}_1, \mathbf{\Omega}_2, \tau)\right|^2\right] \quad (5)$$

is the bi-direction-delay power spectrum of the dth path component.

3. DISPERSIVE PATH PARAMETER ESTIMATORS

In this section we briefly review two proposed high-resolution techniques for estimating dispersive path components, namely the clustering approach, which represents dispersive path components with a sum of specular components, and the density approach, which models the power spectral densities of individual dispersive path components by means of a parametric family of density functions.

3.1. Clustering Approach

In the clustering approach the power spectrum of the dth dispersive path component of (5) is represented by N_d specular components:

$$P_d(\mathbf{\Omega}_1, \mathbf{\Omega}_2, \tau) = \sum_{j=1}^{N_d} P_{d,j} \cdot \delta(\mathbf{\Omega}_1 - \mathbf{\Omega}_{1,d,j}) \cdot \\ \delta(\mathbf{\Omega}_2 - \mathbf{\Omega}_{2,d,j}) \cdot \delta(\tau - \tau_{d,j}), \quad (6)$$

where $P_{d,j}$, $\mathbf{\Omega}_{1,d,j}$, $\mathbf{\Omega}_{2,d,j}$ and $\tau_{d,j}$ are respectively the power, the DoD, the DoA, and the delay of the jth specular component of the dth dispersive path component, and $\delta(\,\cdot\,)$ denotes the Dirac delta function. The number of specular components N_d may depend on d. The nominal and spread parameters of each dispersive path component are calculated as

$$\bar{\eta}_d = \frac{\sum_{j=1}^{N_d} P_{d,j}\eta_{d,j}}{\sum_{j=1}^{N_d} P_{d,j}} \quad (7)$$

$$\sigma_{\eta_d} = \sqrt{\frac{\sum_{j=1}^{N_d} P_{d,j}(\eta_{d,j} - \bar{\eta}_d)^2}{\sum_{j=1}^{N_d} P_{d,j}}}, \quad (8)$$

where η may stand for ϕ_1, θ_1, ϕ_2, θ_2, or τ.

In the clustering approach estimation of dispersive path components is performed in two stages. In the first stage, the bi-direction-delay spread function is represented as a sum of specular components:

$$h(\mathbf{\Omega}_1, \mathbf{\Omega}_2, \tau) = \sum_{n=1}^{N} h_n \cdot \delta(\mathbf{\Omega}_1 - \mathbf{\Omega}_{1,n}) \cdot \\ \delta(\mathbf{\Omega}_2 - \mathbf{\Omega}_{2,n}) \cdot \delta(\tau - \tau_n). \quad (9)$$

A high-resolution estimator, usually based on the SAGE algorithm, is used to extract the parameters h_n, $\mathbf{\Omega}_{1,n}$, $\mathbf{\Omega}_{2,n}$, and τ_n, $n = 1 \ldots N$ from each channel realization. In the second stage, the estimated specular components gathered from N_c realizations, undergo a selection process and those components retained are grouped into clusters. The components allocated to one cluster form an estimate of its power spectrum

(6). The corresponding component parameters are plugged in (7) and (8) to obtain estimates of the nominal values and spreads of the cluster in the dispersion dimensions.

The various implementations of the clustering approach found in the literature differ in the pruning and grouping methods in the second stage and in the investigated dispersion dimensions. In the sequel we shortly review these implementations. All of them consider horizontal-only propagation, i.e., a direction is specified by its azimuth only: $\mathbf{\Omega} = [\cos(\phi), \sin(\phi)]^T$.

In [13] static multiple-input multiple-output (MIMO) indoor channel measurements are processed to assess dispersion in azimuth of arrival (AoA) and azimuth of departure (AoD). The measurement data is partitioned into subsets collected in frequency sub-bands and using specific sub-arrays. The sub-bands and sub-arrays are selected in such a way that the channel transfer functions corresponding to any two subsets of data are nearly uncorrelated. Several thousand of specular path components are estimated from these subsets. The estimated components are selected and grouped into clusters by means of a visual inspection procedure relying on a computed bi-azimuth Bartlett spectrum.

In [11, 14] delay-AoA dispersion in large office, foyer, and laboratory environments is experimentally investigated from single-input multiple-output (SIMO) measurement data. The delay-AoA spread function reconstructed from estimated specular components is convolved with either a 2-dimensional Gaussian density kernel [11] or a Hanning window [14]. Pruning and grouping of the estimated components are carried out by visual inspection of the squared-magnitude of the smoothed delay-AoA spread functions.

The clustering approaches discussed so far rely all on visual inspection by a "trained" person. This step introduces a significant amount of heuristic. Indeed, the individual decisions of the trained person regarding the pruning and grouping of the specular path components heavily influence the results and make them difficult to compare. Moreover, the visual cluster identification is time-consuming and therefore inappropriate for processing large amounts of measurement data. A framework for automatic clustering of the estimated specular path components, using the k-means algorithm, is introduced in [15] and applied in [12].

3.2. Density Approach

In the density approach the power spectral density (5) of path component d is recast according to

$$P_d(\mathbf{\Omega}_1, \mathbf{\Omega}_2, \tau) = P_d \cdot f(\mathbf{\Omega}_1, \mathbf{\Omega}_2, \tau; \boldsymbol{\theta}_d), \qquad (10)$$

where P_d denotes the average power of the dth component. The normalized bi-direction-delay power spectral density $f(\mathbf{\Omega}_1, \mathbf{\Omega}_2, \tau; \boldsymbol{\theta}_d)$ is an element of a family of density functions indexed by the parameter vector $\boldsymbol{\theta}_d$.

In [9] the constrained maximum-entropy principle is proposed to select the family. More specifically, the family is the solution of the problem of finding the density function maximizing the entropy, under the constraint that density's first and second moments are specified. Various solutions for various subsets of dispersion dimensions have been published [9, 10]. They all lead to density functions of the von-Mises-Fisher kind. The investigations performed in [9] aim at experimentally characterizing bi-azimuth and delay dispersion. Moreover, horizontal-only propagation is assumed. The maximum-likelihood estimator of the parameters $\mathbf{\Theta} = [\boldsymbol{\theta}_1, \ldots \boldsymbol{\theta}_D]$ is approximated using the SAGE algorithm [9]. The method is applied in Section 4.2. The reader is referred to [9] for a detailed description of the family of density functions and the maximum-likelihood estimator.

For the sake of completeness it should be mentioned that early implementations of the density approach have been already proposed, however with a different application in mind [5–8].

Table 1. Parameter settings for the simulations.

f_c = 5.25 GHz	$\bar{\tau}$=15 ns	σ_τ=3.5 ns
Bandwidth = 100 MHz	$\bar{\phi}_1$=0°	σ_{ϕ_1}=11°
SNR=30 dB, N_c=4	$\bar{\phi}_2$=0°	σ_{ϕ_2}=2°

4. NUMERICAL AND EXPERIMENTAL RESULTS

The density and clustering approaches are compared by simulation in Section 4.1. In Section 4.2 the density approach is applied to measurement data. These obtained experimental results are compared to empirical values found in literature in Section 4.3 and parameter settings of stochastic models in Section 4.4.

4.1. Accuracy of Spread Estimators

We consider the scenario described by the the settings in Table 1 for the Monte Carlo simulation. The arrays at the transmitter and the receiver have the same response, which coincides with that of the 9-element circular array used to collect the measurement data processed in Section 4.2 and [9]. In each simulation run the signal model described in Section 2 is used to generate the signal contributed by one dispersive path component with dispersion characteristics reported in Table 1. The density estimator described in [9] is applied to estimate the parameters of the bi-azimuth-delay power spectrum.

We now describe the generic clustering approach considered for the simulations. This approach applies a pruning procedure similar to the clustering approaches described in Section 3.1, and therefore is equivalent to share their behaviors. The SAGE algorithm [16] processes the signals generated in each run to estimate a certain fixed number N of specular path components, i.e. to compute an estimate of (9); N_c consecutive runs are processed in this way to obtain $N_c \cdot N$ specular component estimates. Pruning of the path components is conducted as follows: Among the $N_c \cdot N$ components, only those with power larger than a given dynamic range (DR) with respect to the maximum component power are retained. The power of a component is its squared absolute weight. The

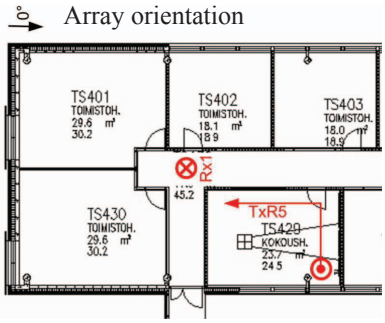

Fig. 2. The investigated environment [17, Scenario TxR5].

retained set of path components form an estimate of (10). Estimates of the nominal azimuth and azimuth spread are computed by plugging the parameters of these estimates in (7) and (8). The average of 100 azimuth spread estimates is depicted in Fig. 3 versus N for different DRs. Notice that no component is discarded when DR=∞.

The results depicted in Fig. 3 show that the choice of the DR and the parameter N heavily influence the behavior of the clustering approach. For instance for the large true spread in Fig. 3 (a) with N=4 and DR$\geq$18 dB, the cluster based method underestimates the spread. For a small true spread as in Fig. 3 (b), the same setting leads to overestimation of the spread. This example clearly exposes the difficulty in optimizing the setting of DR; the appropriate setting depends on the true spread value as well as the number of components N extracted for a cluster – both of which are unknown in real measurements. Notice that N=4 is a typical value returned by the high-resolution estimation algorithms used in the clustering approaches.

4.2. Component Spreads of Measured Data Estimated with the Density Approach

Measurement data collected in an office environment with a channel sounder operating with the settings reported in the first column in Table 1 are used to experimentally assess the performance of the density estimator. A map of the investigated environment including the transmitter trajectory (in red) and the receiver position is shown in Fig. 2. The transmitter was pushed with an approximate speed of 0.5 m/s. The data collected within the first N_c=20 measurements from the instant the transmitter started moving are considered in this investigation. The traveled distance between the data acquisitions of 20 consecutive measurements is approximately 14 cm. We assume that the propagation conditions are approximately constant over this distance. A more detailed explanation of the measurement campaign, referred to as TxR5, can be found in [17]. The estimator described in [9] is used to estimate the bi-azimuth-delay power spectral density of individual path components.

Due to the limited bandwidth of the sounding signal, we set the minimum delay spread to be estimated to one tenth of the sample interval, i.e. 0.5 ns. Moreover, the coupling coefficients between the spreads in delay and azimuths are

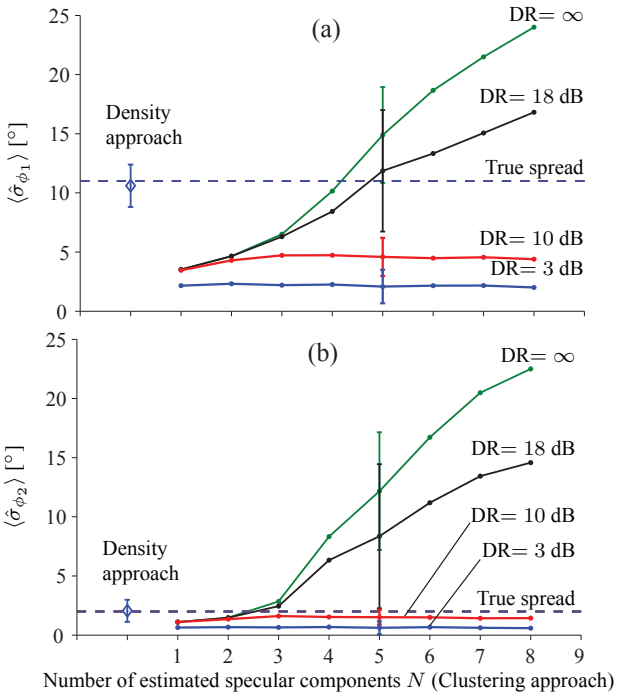

Fig. 3. Comparison of the estimated AoD spread (a) and AoA spread (b) computed with the density estimator and the clustering method. The clustering method uses different settings of the number of specular components N and DR. The error bars indicate the standard deviations of the estimates.

only considered when the delay spread is strictly larger than this value. To avoid numerical problems, we set the maximum absolute value of the coupling coefficients between AoA and AoD to 0.9 instead of 1.

The SAGE algorithm [9] estimates D=8 path components, using 6 iterations (per component). The dynamic range of the component power is set to 30 dB, i.e. the components found with power 30 dB less than the largest component power are discarded. The results are reported in Table 2. In this table, $\hat{(\cdot)}$ denotes an estimate of the parameter given as an argument. It can be seen that some of the dispersed components are highly concentrated with small delay spread ($\leq$0.5 ns).

Bi-azimuth Bartlett spectra computed at different delay bins from the sample covariance matrix ($\widehat{\mathbf{\Sigma}}$) are reported in the first column of Fig. 4. The third column depicts the contour plots of the bi-azimuth power spectra ($\hat{P}(\phi_1, \phi_2, \tau)$) derived from the estimated bi-azimuth-delay power spectrum computed with the density approach. Finally, the second column depicts the bi-azimuth Bartlett spectra computed from the covariance matrix ($\mathbf{\Sigma}(\widehat{\mathbf{\Theta}})$) reconstructed from the estimated bi-azimuth-delay power spectrum. Most of the estimated components have their delays in the three considered bins. The shape and size of the corresponding footprints of the dispersive components in two adjacent Bartlett spectra are very similar. The estimated component power densities are much more concentrated than the corresponding footprints in the Bartlett spectra.

Table 2. Parameter estimates of the power spectral density of individual components.

d	$\hat{P}_d$ [dB]	$\hat{\sigma}_{\tau,d}$ [ns]	$\hat{\sigma}_{\phi_1,d}$ [°]	$\hat{\sigma}_{\phi_2,d}$ [°]	$\hat{\rho}_{\phi_1,\tau,d}$	$\hat{\rho}_{\phi_2,\tau,d}$	$\hat{\rho}_{\phi_1,\phi_2,d}$
1	−54	≤ 0.5	3.7	3.0	–	–	−0.90
2	−56	≤ 0.5	5.9	6.0	–	–	0.39
3	−56	1.8	14.7	0.7	−0.42	0.06	0.39
4	−59	0.9	6.0	3.5	0.35	0.06	−0.90
5	−60	≤ 0.5	5.7	14.1	–	–	0.82
6	−58	≤ 0.5	3.5	4.1	–	–	−0.90
7	−59	3.5	13.5	3.2	0.40	−0.01	−0.79
8	−64	5.3	2.9	8.0	−0.42	−0.01	−0.90
avg.		1.7	7.0	5.3			
std.		1.8	4.5	4.1			

–: values are neglected due to small delay spread estimates.

4.3. Comparison of Experimentally Obtained Path Component Spreads

The upper part of Table 3 summarizes published estimates of path-component spreads experimentally obtained using the clustering methods described in Section 3, as well as the results presented in [18]. Minima, maxima and means of average values computed over different environments and positions are reported. The number of dispersive components D and the number of specular components N_d are average values as well. The results presented in this paper using the density approach are summarized in Table 3 for comparison.

It can be observed from Table 3 that all cluster approaches lead to larger delay spread compared to the values obtained with the density approach. The same observation holds for the minimum azimuth spreads, apart from [13]. It appears that the reported maximum azimuth spreads are in accordance for both approaches. All clustering approaches but [13] lead to larger average values for the azimuth spreads. The range and average of azimuth spread estimates presented in [13] are more or less in agrement with the results obtained with the density approach. Fig. 8 in reference [13] shows that this "manual" clustering approach leads to an unbiased estimator when the true azimuth spread is lower that $5°$. Above $5°$, the estimator under estimates the true spread.

Although clear and definitive conclusions can be hardly drawn from Table 3, the observed trend is that the considered clustering approaches but [13] tend to lead to larger spreads compared to the density approach. Two theses are proposed that can explain this discrepancy: 1) The spread values are obtained from experimental investigations of delay-azimuth dispersion in specific indoor channels [11, 13, 14, 18]. Some path components with small spreads that might be resolvable in the bi-azimuth delay dimensions, i.e. with the density approach in [9], might appear as one component with larger spreads when resolved in the delay-azimuth dimensions only; 2) As discussed in Section 4.1 over-estimation of the spreads might be a result of the inherent behavior of the clustering approach.

4.4. Component Spreads in Standard Models, Revisited

The settings of the spread parameters of two widely used indoor channel models supporting per-cluster direction and delay spreads are included in the bottom part of Table 3. The reader is referred to the provided references for a detailed description of these models. The 802.11 Tgn channel Model B (typical large open space and office environments, NLOS conditions, and 100 ns rms delay spread) [19] is based on a tapped delay line with inter-tap spacing of 10 ns. All cluster taps exhibit the same azimuth spread. The Winner II Model scenario A1 (Indoor Office) [20] relies on a geometric cluster representation. A less complex implementation, based on a "cluster delay line" in which each tap is considered as a cluster, is suggested too. The inter-tap spacing is 5 ns. The tap spacings of these two models are of the same order as the resolution of the sounding equipments used to collect the measurement data based on which the results depicted in the top part of Table 3 are obtained. For instance, the sounder used to gather the data processed in Section 4.2 has a 10 ns resolution. We conclude from this observation that the taps in the 802.11 Tgn and Winner II models can be viewed as dispersive path components in the sense described in this paper.

The component spreads specified in the Winner II Model A1 rely partly on the experimental results of [12, 13] and correspond to mean values reported in these references. They are in accordance with the experimental values found in Table 2. The setting of spread values of the 802.11 Tgn Model B has been selected based on the results of [11, 14, 18]. The specified spread values are significantly larger that those given in Table 2. The over-estimation trend of the clustering approach mentioned in the previous section might partly explain this observation.

The COST273 [21] model supports dispersion in bi-azimuth and delay of so-called clusters of path components. The values provided for the cluster spreads in picocell envi-

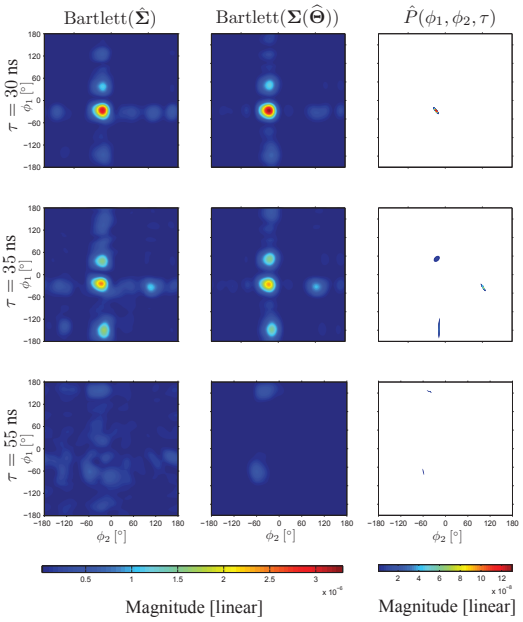

Fig. 4. Bi-azimuth spectra versus delay in an indoor environment. (for more details see Section 4.2)

Table 3. Selected published values of spread parameters for indoor environments.

Ref.	D	N_d	σ_τ [ns]			$\sigma_{\phi,1}$ [°]			$\sigma_{\phi,2}$ [°]		
			min	max	avg.	min	max	avg.	min	max	avg.
Experimental Results											
Table 2	8.0		$\leq$0.5	5.3	1.7	2.9	14.7	7.0	0.7	14.1	5.3
[11]	8.0	5.0	13.4	37.9	–				3.3	9.5	–
[12]	11.0	8.0	6.0	10.0	7.8	10.8	19.0	15.7	9.3	14.9	12.2
[13]	8.8					2.4	11.1	5.2	2.6	8.2	5.5
[14]	4.5								5	25	13.7
[18]	4.0								22.0	26.0	–
Settings in Two Commonly Used Channel Models											
Winner II [20]	13.3	20.0	6.0	10.0	–	5.0	6.0	–	5.0	13.0	–
802.11 Tgn [19]	9.0					14.4	25.4	–	14.4	25.2	–

ronments [21] are usually much larger, e.g. σ_τ=300 ns and $\sigma_{\phi,2}$=30°. This indicates that these clusters cannot be identified with the dispersive components described in Section 3. Clusters defined in the COST273 sense appear to be clusters of such dispersive components. Further studies are, however, necessary to clarify this conjecture.

5. DISCUSSION AND CONCLUSION

The paper addresses some important aspects related to the high-resolution estimation of dispersion in radio channels. To this end, we have studied the behavior and performance of two approaches for estimating the spreads of individual path components in indoor environments, namely the clustering approach and the density approach.

The reported simulation results reveal the shortcomings of the clustering approach, when it is used to estimate component spreads. The method, combined with a trained visual inspection, seems to work appropriately [13]. The heuristic and manual steps in the selection of the clusters, however, make it difficult to accept it as a qualitative tool. The simulation results also show that the density approach is an efficient alternative to the clustering approach. The review of experimental component spreads presented in Section 4.3 demonstrates the difficulty of comparing similar experimental qualities, when they are gathered in different environments and processed using different methods. It is conjectured that some of the spread values reported in the literature are too large to characterize bi-azimuth-delay dispersion of path components. Two possible theses have been formulated to explain this effect: 1) the intrinsic behavior of the clustering approach and 2) the fact that the experimental investigations were limited to azimuth-delay dispersion of the radio channel, so another additional dimension, i.e. azimuth of departure, was not exploited to resolve path components.

Some of the reported experimental results have been used to specify the settings of the component spreads of the Winner II Model A1 (Indoor Office) and the 802.11 Tgn Model B (typical NLOS large open space and office environments). The discussion shows that the values selected in the parameter settings of these models are as reliable as the estimators used to extract the empirical information based on which these parameters are selected. This – apparently obvious observation – stresses the necessity to validate channel parameter estimators in order to clearly understand their behavior and performance.

The discussions in Section 4.3 and Section 4.4 rely on limited experimental evidence gathered from a small set of results obtained with the density approach. However, further experimental observations not reported here confirm the presented theses. Nevertheless, a more comprehensive study is necessary in order to definitely confirm them, and especially to confirm the conjecture that path component spreads in bi-direction and delay are typically smaller that commonly believed.

6. REFERENCES

[1] K.-H. Li, M.A. Ingram, and A. Van Nguyen, "Impact of Clustering in Statistical Indoor Propagation Models on Link Capacity," *IEEE Trans. Commun.*, vol. 50, no. 4, pp. 521–523, 2002.

[2] Z. Tang and A. S. Mohan, "Impact of Clustering in Indoor MIMO Propagation Using a Hybrid Channel Model," *EURASIP J. Appl. Signal Process.*, vol. 2005, no. 1, pp. 1698–1711, 2005.

[3] T. Betlehem, T.D. Abhayapala, and T.A. Lamahewa, "Space-Time MIMO Channel Modelling Using Angular Power Distributions," in *Proc. 7th Australian Commun. Theory Workshop*, 2006, pp. 165–170.

[4] M. Bartlett, "Smoothing periodograms from time series with continuous spectra," *Nature*, vol. 161, 1948.

[5] M. Bengtsson and B. Ottersten, "Low-Complexity Estimators for Distributed Sources," *IEEE Trans. Signal Process.*, vol. 48, no. 8, pp. 2185–2194, 2000.

[6] T. Trump and B. Ottersten, "Estimation of Nominal Direction of Arrival and Angular Spread Using an Array of Sensors," *Signal Process.*, vol. 50, no. 1-2, pp. 57–69, 1996.

[7] O. Besson and P. Stoica, "Decoupled Estimation of DOA and Angular Spread for a Spatially Distributed Source," *IEEE Trans. Signal Process.*, vol. 48, no. 7, pp. 1872–1882, 2000.

[8] C. Ribeiro, A. Richter, and V. Koivunen, "Joint Angular- and Delay-Domain MIMO Propagation Parameter Estimation Using Approximate ML Method," *IEEE Trans. Signal Process.*, vol. 55, no. 10, pp. 4775–90, 2007.

[9] X. Yin, T. Pedersen, N. Czink, and B. H. Fleury, "Parametric Characterization and Estimation of Bi-Azimuth and Delay Dispersion of Path Components," in *Proc. of the First European Conf. on Antennas and Progation (EuCAP)*, Acropolis, Nice, France, November 2006.

[10] X. Yin, L. Liu, and et al., "Modeling and estimation of the direction-delay power spectrum of the propagation channel," in *Proc. 3rd Int. Symposium on Commun., Control and Signal Process. ISCCSP 2008*, Mar. 2008, pp. 225–230.

[11] C.-C. Chong, C.-M. Tan, and et al., "A New Statistical Wideband Spatio-Temporal Channel Model for 5-GHz Band WLAN Systems," *IEEE J. Sel. Areas Commun.*, vol. 21, no. 2, pp. 139–150, 2003.

[12] N. Czink, E. Bonek, and et al., "Parameterizing Geometry Based Stochastic MIMO Channel Models From Measurements Using Correlated Clusters," in *Proc. of the ITG Workshop on Smart Antennas*, Vienna, Austria, February 2007.

[13] N. Czink, X. Yin, et al., "Cluster Characteristics in a MIMO Indoor Propagation Environment," *IEEE Trans. Wireless Commun.*, vol. 6, no. 4, pp. 1465–75, 2007.

[14] Kai Yu, Q. Li, D. Cheung, and C. Prettie, "On the Tap and Cluster Angular Spreads of Indoor WLAN Channels," in *Proc. of the 59th IEEE Veh. Technol. Conf. (VTC)*, 2004, vol. 1, pp. 218–222 Vol.1.

[15] N. Czink, P. Cera, and et al., "A Framework for Automatic Clustering of Parametric MIMO Channel Data Including Path Powers," in *Proc. of the 64th IEEE Veh. Technol. Conf. (VTC)*, 2006, pp. 1–5.

[16] B.H. Fleury, M. Tschudin, and et al., "Channel Parameter Estimation in Mobile Radio Environments Using the SAGE Algorithm," *IEEE J. Sel. Areas Commun.*, vol. 17, no. 3, pp. 434–450, March 1999.

[17] N. Czink, *The Random-Cluster Model - A Stochastic MIMO Channel Model for Broadband Communication Systems of the 3rd Generation and Beyond*, Ph.D. thesis, Vienna University of Technology, 2007.

[18] Q.H. Spencer, B.D. Jeffs, and et al., "Modeling the statistical time and angle of arrival characteristics of an indoor multipath channel," *IEEE J. Sel. Areas Commun.*, vol. 18, no. 3, pp. 347–360, 2000.

[19] V. Erceg, L. Schumacher, P. Kyritsi, and et al., "TGn Channel Models," Tech. Rep. IEEE P802.11, Wireless LANs IEEE 802.11-03/940r4, Garden Grove, Calif, USA, May 2004.

[20] P. Kyösti, J. Meinilä, and et al., "WINNER II Channel Models D1.1.2 V1.1," Tech. Rep. IST-4-027756 WINNER II, IST Winner II Project, 11 2007.

[21] L. M. Correia, *Mobile Broadband Multimedia Networks: Techniques, Models and Tools for 4G*, Academic Press, 5 2006.